

1   **Experimental evidence for rapid genomic adaptation to a new niche in an adaptive radiation**

2

3   David A. Marques<sup>1,2\*</sup>, Felicity C. Jones<sup>3,4</sup>, Federica Di Palma<sup>5</sup>, David M. Kingsley<sup>3</sup> & Thomas E.  
4   Reimchen<sup>1</sup>

5

6   <sup>1</sup>Department of Biology, University of Victoria, PO Box 3020, Victoria, BC, V8W 3N5, Canada

7   <sup>2</sup>current address: Institute of Ecology and Evolution, University of Bern, Switzerland and Department  
8   of Fish Ecology and Evolution, Eawag: Swiss Federal Institute of Aquatic Science and Technology,  
9   Kastanienbaum, Switzerland.

10   <sup>3</sup>Stanford University School of Medicine, Department of Developmental Biology, 279 Campus Dr,  
11   Beckman Center B300, Stanford, CA, USA

12   <sup>4</sup>Friedrich Miescher Laboratory of the Max Planck Society, 72076 Tübingen, Germany

13   <sup>5</sup>Earlham Institute and University of East Anglia, Department of Biological Sciences, Norwich, UK

14

15   \*Corresponding author: David A. Marques, david.marques@eawag.ch

16

17   **A substantial part of biodiversity is thought to have arisen from adaptive radiations in which**  
18   **one lineage rapidly diversified into multiple lineages adapted to many different niches.**  
19   **However, selection and drift reduce genetic variation during adaptation to new niches and may**  
20   **thus prevent or slow down further niche shifts. We tested whether rapid adaptation is still**  
21   **possible from a highly derived ecotype in the adaptive radiation of threespine stickleback on the**  
22   **Haida Gwaii archipelago, Western Canada. In a 19-years selection experiment, we let giant**  
23   **stickleback from a large blackwater lake evolve in a small clearwater pond without vertebrate**  
24   **predators. 56 whole genomes from the experiment and 26 natural populations revealed that**  
25   **adaptive genomic change was rapid in many small genomic regions and encompassed 75% of**  
26   **the adaptive genomic change between 12,000 years old ecotypes. Adaptive genomic change was**  
27   **as fast as phenotypic change in defence and trophic morphology and both were largely parallel**  
28   **between the short-term selection experiment and long-term natural adaptive radiation. Our**  
29   **results show that functionally relevant standing genetic variation can persist in derived adaptive**  
30   **radiation members, allowing adaptive radiations to unfold very rapidly.**

31   The colonization of a new habitat or niche requires rapid adaptation to multiple environmental  
32   challenges, i.e. to ‘multifarious’ divergent selection. This is most dramatic in adaptive radiations,  
33   where rapid successions of niche and habitat shifts occur within a lineage<sup>1-3</sup>. However, most adaptive  
34   radiations started thousands of generations ago and we don’t know whether major phenotypic and  
35   genomic adaptation occurred within the first few generations of colonizing a new habitat, or over  
36   longer time scales and thus how ‘rapid’ adaptive radiations unfold. Adaptation may be instantaneous  
37   when phenotypic plasticity is involved<sup>4,5</sup> or occur over few generations of selection on standing  
38   genetic variation<sup>6,7</sup> or admixture variation<sup>8,9</sup>. Alternatively, adaptation may require time for beneficial  
39   *de novo* mutations to arrive, or genomic adaptation may occur slower than phenotypic adaptation if  
40   rapid phenotypic plasticity is followed by slower genetic assimilation<sup>4,10</sup>. Furthermore, each new  
41   habitat shift will reduce genetic variation through drift and selection and it is unclear whether further

42 adaptation is hampered or slowed down after a first new niche has been colonized in an adaptive  
43 radiation.

44 Evolution experiments and cases of contemporary evolution, such as in biological invasions, may  
45 reveal the speed of phenotypic and genomic adaptation<sup>11,12</sup>. However, many ‘evolve and re-sequence’  
46 experiments and contemporary evolution studies focussed on single selective agents instead of  
47 multifarious fitness landscapes<sup>13-21</sup>, or phenotypic and genomic adaptation have been studied in  
48 isolation<sup>22-25</sup>. Only few examples of phenotypic and genomic contemporary evolution under  
49 multifarious divergent selection have been documented, such as marine threespine stickleback  
50 (*Gasterosteus aculeatus*) colonizing freshwater habitats in artificial and natural selection  
51 experiments<sup>25-28</sup>, showing widespread parallel genomic and phenotypic adaptation compared to  
52 thousands of generations older natural populations<sup>7,29</sup>.

53 Here, we quantify the speed of genomic adaptation to multifarious divergent selection in a 19 years  
54 selection experiment, starting from a phenotypically highly derived adaptive radiation member, and  
55 compare rates of phenotypic and genomic change. We expand on a long term investigation of the  
56 adaptive radiation of threespine stickleback from the Haida Gwaii archipelago off Western Canada<sup>30</sup>,  
57 where stickleback have colonized multiple watersheds independently and adapted to diverse  
58 freshwater habitats including lakes, ponds and streams with vastly divergent biophysical features,  
59 predator and parasite communities following glacial retreat ~12,000 years ago<sup>31-34</sup>. Phenotypic  
60 variation in defensive armour<sup>35-39</sup> such as dorsal and pelvic spines, pelvic girdle and lateral plates, and  
61 in trophic morphology<sup>31,39,40</sup> such as in body shape, gape and gill rakers, can be largely explained by  
62 three main predictors: predation regime, light spectrum, and lake size<sup>30</sup>.

63 A selection experiment along these three axes of selection was initiated by T.E.R. in 1993: he  
64 transplanted 100 adult stickleback from a large, deep, dystrophic, blackwater lake (Mayer Lake) with  
65 vertebrate-dominated predation into a small, shallow, eutrophic, previously unoccupied clearwater  
66 pond (Roadside Pond) dominated by invertebrate predators<sup>41</sup>. Mayer Lake contains some of the most  
67 derived freshwater stickleback, maximally divergent from the ancestral marine phenotype and  
68 occupying the extreme morphospace edge of the Haida Gwaii adaptive radiation<sup>30</sup>: 8-10 cm long,  
69 melanistic ‘giants’ with highly developed predator defence and adaptations to limnetic foraging<sup>42,43</sup>,  
70 low levels of phenotypic variance<sup>31</sup> but similar levels of genetic variation as other Haida Gwaii  
71 populations<sup>34,44</sup>. After evolving for 16 years in the new selective regime, six predator defence, four  
72 feeding morphology traits and eye size evolved in the expected direction (Fig. 1a), encompassing  
73 ~30% of the morphological distance between natural stickleback populations from large lakes and  
74 small ponds<sup>41</sup> (Fig. 2a). Life history changed from two to one year age of first reproduction and  
75 melanism was reduced<sup>41,45</sup>. Phenotypic evolution was fast with on average 0.15 (0-0.25) *haldanes*  
76 over 11 generations, assuming an average generation time of 1.5 years<sup>41</sup>. While strong change in the  
77 first generation for four traits suggested phenotypic plasticity, other traits showed slower change  
78 suggesting genetic change. We use whole genomes from 26 natural populations, including the source  
79 Mayer Lake (N = 12), and the transplant population Roadside Pond (N = 11) sampled after evolving  
80 for 19 years or 13 generations in the new habitat, to identify the speed and targets of genomic  
81 adaptation and the extent of genomic parallelism with the Haida Gwaii adaptive radiation.

## 82 Results

83 **Moderate genome-wide change, but strong change in many small genomic regions.** Giant  
84 stickleback evolving for 13 generations in a new habitat showed only moderate genome-wide change  
85 (Fig. 1b-c), but strong change in many small genomic regions (Fig. 3-4). Allele frequencies (AF)  
86 changed on average by 11.4 % (weighted mean  $|\Delta AF|$ , Fig. 1c), leading to a genomic ‘background’  
87 differentiation between Mayer Lake and Roadside Pond of  $F_{ST} = 0.057$  for autosomes and  $F_{ST} = 0.107$   
88 for the female sex chromosome (weighted pairwise  $F_{ST}$ , Fig. 1b). Compared to differentiation

89 observed between natural, postglacial populations, 13 generations of evolution encompassed 41% of  
90 the differentiation between lake and stream ecotypes and 22% of the differentiation between  
91 stickleback from the large lake Mayer Lake and three independently colonized small ponds on Haida  
92 Gwaii (Fig. 2c). Similarly, mean pairwise divergence ( $D_{XY}$ ), reflecting the sorting of polymorphic,  
93 ancient divergent genomic regions between populations on these short time scales, increased  
94 marginally ( $D_{XY, \text{within populations}} = 0.0037$ ,  $D_{XY, \text{between Mayer-Roadside}} = 0.0038$ ,  $t_{183} = -2.88$ ,  $P = 0.004$ ) and  
95 encompassed 20% of the divergence between naturally occurring lake and stream ecotypes and 9% of  
96 the divergence between Mayer Lake and small ponds (Fig. 2b, Supplementary Results).

97 The transplant of giant Mayer Lake stickleback to Roadside Pond led to a slight loss of genetic  
98 diversity and a prominent, genome-wide distortion of the site frequency spectrum (SFS, Fig. 1b,  
99 Supplementary Fig. 2a). Mean nucleotide diversity was reduced by 7.4% from  $\pi_{\text{Mayer}} = 0.0047$  to  
100  $\pi_{\text{Roadside}} = 0.0043$  (mean 10kb windows,  $t_{85940} = 22.56$ ,  $P < 0.001$ , Fig. 1b), but local diversity across  
101 the genome between both populations remained strongly correlated (Pearson's  $r = 0.92$ , linear  
102 regression  $F_{2,43444} = 89,485$ ,  $P < 0.001$ , Supplementary Fig. 3). The distribution of Tajima's D was  
103 shifted to a positive mean from  $T_{D, \text{Mayer}} = -0.27$  to  $T_{D, \text{Roadside}} = 0.60$  (mean 10kb windows,  $t_{85623} = -$   
104 197.11,  $P < 0.001$ , Fig. 1b), indicating the loss of rare alleles relative to common alleles evident from  
105 the observed 1D-SFS (Supplementary Fig. 2a), but Tajima's D remained correlated across the genome  
106 (Pearson's  $r = 0.53$ , linear regression  $F_{2,43444} = 17,277$ ,  $P < 0.001$ , Supplementary Fig. 3).

107 **Genomic footprints of divergent selection are widespread in the genome.** Genome-wide average  
108 changes such as diversity loss and a shifted Tajima's D distribution are likely a product of  
109 demographic history, while localized changes in the genome may reflect footprints of selection. To  
110 distinguish the two, we reconstructed the demographic history of Mayer Lake and Roadside Pond  
111 stickleback (see Methods). The demographic model best fitting the observed 2D-SFS features a  
112 bottleneck ~8,200 generations ago, translating to ~12,300 years, in line with the postglacial  
113 colonization of Mayer Lake and also recovered the observed population growth of the Roadside Pond  
114 population following the transplant<sup>41</sup> (Supplementary Fig. 2). We identified signatures of divergent  
115 selection between Mayer Lake and Roadside Pond in the genome from outliers for differentiation  
116 ( $F_{ST}$ ), change in diversity ( $\Delta\pi$ ) or Tajima's D ( $\Delta T_D$ ) and haplotype-based selection statistics (iHS,  
117 XPEHH) against neutral expectations from demographic history by simulating genomic data under  
118 the best-fitting demographic model (Supplementary Fig. 3, see Methods). The simulations reproduced  
119 both the observed diversity loss and positive shift in Tajima's D (Supplementary Fig. 4).

120 Traces of divergent selection among the habitats are widespread across the genome: we found 77  
121 outlier regions distributed across 15 chromosomes, covering 15.73Mb or 3.6% of the genome (Figs.  
122 3-4, Supplementary Figs. 5-19 and Table 1), exceeding expectations from simulated neutral genomic  
123 data (0.16-0.25% of the genome). Outlier regions varied in size between 30kb and 940kb (mean =  
124 204kb, median = 160kb). Three quarters of outlier regions show patterns indicating a near-complete,  
125 past selective sweep in Mayer Lake, followed by a quick rise of the previously disfavoured allele to  
126 high / intermediate frequency in Roadside Pond: negative Tajima's D in Mayer Lake, positive  
127 Tajima's D in Roadside Pond, negative XPEHH, significant differentiation and exceptional allele  
128 frequency shifts between the populations (Fig. 4, Supplementary Figs. 5-19). The remaining quarter of  
129 outlier regions shows an opposite pattern indicating a selective sweep in Roadside Pond but not in  
130 Mayer Lake: reduced Tajima's D and diversity in Roadside Pond, significant H12 patterns for  
131 Roadside Pond and a positive XPEHH (Supplementary Figs. 6-19). Both patterns are in agreement  
132 with divergent selection between the habitats in the experiment.

133 We computed linkage disequilibrium (LD) between outlier regions to test whether divergent selection  
134 acted on a single region genomic with others hitchhiking, or whether multiple regions responded  
135 independently to divergent selection. Significant inter-chromosomal LD was found mainly between  
136 outlier regions in the Mayer Lake population (Supplementary Fig. 20), indicating that several regions

137 involved in divergent selection in the experiment are not segregating fully independently in the source  
138 population. In the transplant population Roadside Pond however, we found only seven significant  
139 inter-chromosomal associations (Supplementary Fig. 20), suggesting that while outlier regions on  
140 different chromosomes responded largely independently to divergent selection in the experiment,  
141 some uncertainty remains about the exact number of independently selected regions.

142 Adaptive differentiation, defined as the top 5% single SNP  $F_{ST}$  estimates from each genomic outlier  
143 region, ranged from  $F_{ST} = 0.25$  to  $F_{ST} = 0.76$  with a mean of  $F_{ST} = 0.44$ . Allele frequency change at  
144 these SNPs ranged from  $|\Delta AF| = 18\%$  to  $|\Delta AF| = 81\%$  with a mean of  $|\Delta AF| = 51\%$ , which under a  
145 model of purely selection-driven change would correspond to selection coefficients between  $s = 0.24$   
146 and  $s = 1$  with mean  $s = 0.62$ . Compared to naturally evolved, postglacial ecotypes, genomic adaptive  
147 differentiation after only 13 generations of evolution in a new ‘ecological theatre’ thus encompassed  
148 72% of the degree of adaptive differentiation found between postglacial lake and stream ecotypes<sup>46</sup>  
149 and already exceeds adaptive differentiation found between giant Mayer Lake stickleback and its  
150 corresponding parapatric stream ecotype (Fig. 2d).

151 **Genomic targets and parallel evolution in experiment and adaptive radiation.** We identified  
152 potential targets and sources of divergent selection from overlapping genes and QTL<sup>47</sup> and from  
153 genotype-environment and genotype-phenotype (GE/GP) associations in the Haida Gwaii adaptive  
154 radiation. In the latter, we tested whether genomic variation in each outlier region was associated with  
155 change in phenotypic and ecological properties in the selection experiment and across one marine and  
156 25 freshwater populations on Haida Gwaii (see Methods, Fig. 5). We found 654 QTL overlapping  
157 with outlier regions and 336 candidate genes near the centre of each outlier regions’ selective sweep  
158 signature, but no gene ontology term enrichment (Figs. 4 and 5, Supplementary Figs. 5-19 and Tables  
159 2 and 3). 36 outlier regions showed parallel GE/GP associations (Fig. 5).

160 In line with predation landscape being the most important axis of divergent selection in the adaptive  
161 radiation<sup>30</sup>, 96 QTL and one candidate gene controlling predator deference traits overlap with outlier  
162 regions. Among these are major effect QTL for lateral plate number, dorsal spine, pelvic spine and  
163 pelvic girdle length and many intermediate and minor effect QTL for these traits on additional  
164 chromosomes (Fig. 5, Supplementary Table 2). Remarkably, phenotypic variation in pelvic and dorsal  
165 spine length across the Haida Gwaii radiation is associated with genomic variation in eleven and six  
166 outlier regions, respectively, and the phenotypic and genomic change observed in the selection  
167 experiment paralleled the adaptive radiation in ten (pelvic spine) and four (dorsal spine) of these  
168 region (Fig. 5). Variation in plate number across the radiation is associated with genomic variation in  
169 outlier regions IV.i and XVII.f (parallel) and XII.c (non-parallel). While most annotations for  
170 candidate genes did not allow to draw conclusions on defence phenotypes, the *eda* gene in outlier  
171 region IV.e controls lateral plate number<sup>48-50</sup> and several associated traits such as lateral line pattern  
172 and schooling behavior<sup>51,52</sup> (Supplementary Fig. 9). Genetic variation in the *eda* region may be  
173 responsible for the observed reduction of plate number in the selection experiment<sup>41</sup>, while the lack of  
174 an association across the adaptive radiation suggests an involvement of different alleles or genes in  
175 other populations.

176 Variation in light spectrum across the adaptive radiation, the second most important axis of divergent  
177 selection<sup>30</sup>, and the presence of blackwater show many strong, parallel associations with genetic  
178 variation in outlier regions also containing multiple candidate genes involved in (colour) vision (Fig.  
179 5). The six outlier regions most strongly associated with light spectrum in parallel between adaptive  
180 radiation and the selection experiment contain the photoreceptor *opn1sw1* sensitive to UV-light<sup>53</sup>,  
181 *TRPC7* involved in eye physiology<sup>54</sup>, *CACNA2D3* associated with night blindness in humans<sup>55</sup>, the  
182 gene *atp6v1f* involved in retinal pigmentation<sup>56,57</sup>, the nervous system development genes *dennd6b*  
183 and *cers2a* expressed in the eye, lens and retina and *adamts10* involved in lens development<sup>58</sup>. In  
184 addition, outlier region XVII.j shows parallel association with blackwater habitats and contains the

185 blue-light sensitive photoreceptor *opn1sw2*, which we demonstrated previously to be under selection  
186 between blackwater and clearwater habitats both across adaptive radiation and selection experiment<sup>59</sup>.  
187 Repeated adaptation to light spectrum thus has led to multiple signatures of parallel adaptation on  
188 visual perception genes.

189 Many feeding morphology QTL (n = 277) overlap with outlier regions. Jaw length variation in the  
190 adaptive radiation is associated with six outlier regions on five chromosomes, four in parallel and two  
191 non-parallel (Fig. 5). QTL for gill raker number overlap with many outlier regions, with two parallel  
192 associations across the adaptive radiation on chromosomes I and VIII (Fig. 5, Supplementary Table  
193 2). Similarly, many gill raker length QTL overlap with outlier regions, in particular intermediate  
194 effect loci on chromosomes IV and VIII. Also for gill raker spacing, intermediate effect QTL on  
195 chromosomes IV and XX and minor effect QTL overlap with outlier regions. The widespread  
196 genomic architecture of many feeding morphology related traits thus broadly overlaps with genomic  
197 regions under divergent selection. Together with several candidate genes involved in craniofacial  
198 development or various metabolic processes (Supplementary Table 3), these overlaps might reflect  
199 selection on feeding morphology or diet after the shift from a zooplankton to a benthic invertebrate  
200 dominated habitat.

201 Strikingly, we found several candidate genes (*kitlga*, *mc1r*, *gpr25*, *foxd3*, *bnc2*, *STYL2*, *tcta*,  
202 *trappc6bl*, *bloc1s3*, *MYRIP*, *atp6v1f*) in outlier regions involved in pigmentation<sup>57,60-65</sup>. These might  
203 be associated with the decreased melanism found in Roadside Pond stickleback, the loss of red nuptial  
204 coloration or with sexual selection for blue signals in blackwater Mayer Lake<sup>45</sup>. The two first genes  
205 *kitlga* and *mc1r* are well-known targets of divergent selection associated with melanin pigmentation in  
206 stickleback, mammals and reptiles<sup>61,65,66</sup>; and the former overlaps with a large effect QTL for black  
207 pigmentation in other wild stickleback populations<sup>65</sup>. The two genes *STYL2* and *bloc1s3* overlap with  
208 intermediate-effect QTL for red pigmentation<sup>67</sup>. Outlier regions containing these genes do not show  
209 associations with melanism across the Haida Gwaii radiation, nor do melanism-associated regions  
210 across the adaptive radiation contain known pigmentation genes (Fig. 5). Finally, body size shows a  
211 non-parallel association with outlier region XIX.e containing an intermediate-effect QTL for body  
212 size (Supplementary Table 2), while additional, parallel associations are not overlapping with known  
213 QTL or gene function. Many outlier regions are associated with several ecological and phenotypic  
214 traits, other QTL and with geography (Fig. 5). This might reflect modular trait architecture<sup>47,68</sup>,  
215 selection-driven clustering of adaptive variation or indirect associations with correlated ecological and  
216 phenotypic variables across the adaptive radiation.

## 217 Discussion

218 Adaptation of a highly derived threespine stickleback ecotype in the Haida Gwaii adaptive radiation  
219 to the opposite multifarious selection regime along the three major axes of selection resulted in rapid  
220 and widespread adaptive genomic change over only 13 generations. We previously demonstrated  
221 rapid phenotypic change in the selection experiment, encompassing approximately 30% of the  
222 phenotypic divergence of 12,000 year old natural populations<sup>41</sup> (Fig. 1a, 2a). Here, we found that  
223 underlying adaptive genomic variation also responded very fast to divergent selection, with on  
224 average 72% of the expected change occurring in the first 13 generations. The evolutionary rate of  
225 genomic adaptation is thus very high and comparable in speed to contemporary evolution of *Brassica*  
226 *rapa* adapting to drought over 7 generations<sup>18</sup>, showing adaptive differentiation of  $F_{ST} = 0.17-0.44$ , or  
227 to Darwin's Finches undergoing drought-induced ecological character displacement<sup>69</sup>, with a selection  
228 coefficient of 0.59 on a major effect locus. Genomic adaptation in our selection experiment is faster  
229 than in marine stickleback adapting to freshwater habitat over approx. 17 generations in Russia<sup>26</sup>,  
230 where adaptive alleles increased in frequency by 10-50%. Both phenotype, with 0.15 *haldanes* in 12  
231 generations<sup>41</sup>, and adaptive genomic variation with a mean  $F_{ST}$  of 0.46 in 13 generations, thus evolved  
232 at a very rapid rate typical of populations colonizing a new adaptive zone in an adaptive radiation<sup>70</sup>.

233 Rapid adaptation to multifarious divergent selection thus seems to occur similarly fast or faster than  
234 adaptation to a single selective force or with a single major locus as in some of these other examples.

235 Remarkably, the genomic basis of predator defence morphology, colour vision, feeding morphology  
236 and pigmentation overlapped with adaptive genomic change in the selection experiment, including  
237 some ‘master adaptation genes’ such as *eda*, *opnsw1/2*, *kitlg* and *mc1r*, frequently involved in  
238 repeated divergent adaptation of body armor, colour vision and pigmentation<sup>48,49,59,61,65,66,71</sup>. Many of  
239 these regions showed parallel associations with variation in traits and ecosystem variables across the  
240 Haida Gwaii adaptive radiation. This suggests that there was no major gap between phenotypic and  
241 genomic change for most of the diverging traits on the contemporary time scale of the selection  
242 experiment. Although phenotypic plasticity likely contributed to near-instantaneous phenotypic  
243 adaptation for traits such as eye size or gill raker length<sup>41</sup>, our genomic findings suggest that selection  
244 has operated on genetic variation underlying most diverging phenotypic traits. Much of the genetic  
245 variation had to be shared with the Haida Gwaii adaptive radiation as standing genetic variation  
246 within Mayer Lake and across the archipelago, as outlier regions in the selection experiment evolved  
247 in parallel to the radiation in 36 of 77 genomic outlier regions (Fig. 5). Determinism of adaptive  
248 evolution thus is not only prevalent in phenotype<sup>41</sup>, but also in the genome, predicted by the three  
249 major axes of natural selection in the radiation<sup>30</sup>.

250 Genomic parallelism is somewhat surprising, given that a highly derived phenotype in the adaptive  
251 radiation was the source for the selection experiment. Mayer Lake stickleback are vertebrate-  
252 predation, blackwater and zooplankton adapted specialists with little phenotypic variance. It is thus  
253 conceivable that such a specialist would have lacked the necessary standing genetic variation for rapid  
254 adaptation to the opposite extreme ecological theatre. In addition, a bottleneck during the selection  
255 experiment reduced genomic variation by 7%. Indeed, some shared alleles may have been lost during  
256 12,000 years of adaptation to a blackwater lake: strong, but non-parallel associations between  
257 blackwater habitation and outlier regions on several chromosomes in the selection experiment suggest  
258 that different alleles from the adaptive radiation were favoured once the blackwater population had to  
259 re-adapt to the clearwater Roadside Pond (Fig. 5). Nevertheless, the Mayer Lake population still  
260 retained shared genetic variation at many loci for parallel adaptation in feeding morphology, defence  
261 morphology, pigmentation and vision. Genetic variation in Mayer Lake may have been maintained by  
262 disruptive or fluctuating selection within Mayer Lake<sup>37,38,72</sup>, by a large population size in Mayer Lake  
263 (Fig. 5) or occasional introgression of adaptive alleles from adjacent stream ecotypes<sup>46,73</sup> or nearby  
264 lake ecotypes. Linkage disequilibrium between physically unlinked genomic regions containing such  
265 variation in Mayer Lake suggests that standing genetic variation is correlated in some individuals  
266 (Supplementary Fig. 20), compatible with all three hypotheses. Alternatively, bottlenecks during the  
267 colonization of Mayer Lake 12,000 years ago and during the experiment may not have been strong  
268 enough to remove adaptive genetic variation, such as in biological invasions where adaptive potential  
269 is usually not hampered with reductions in genetic diversity of 15-20%<sup>12,74</sup>. Drift during habitat shifts  
270 may thus rarely hamper sequential and rapid colonization of new niches in an adaptive radiation.

271 Our results confirm that natural selection generally overrides historical contingency at the genomic  
272 level in the adaptive radiation of threespine stickleback on Haida Gwaii, in line with phenotypic  
273 patterns<sup>30</sup> and previous genomic results for lake-stream and marine-freshwater divergence<sup>7,26,27,34,46</sup>,  
274 and in spite of bottlenecks upon colonization and strong selection acting on new colonizers. Similar  
275 selection-driven phenotypic and genomic determinism has been found in other adaptive radiations,  
276 based on adaptive introgression or a hybrid swarm origin rather than on standing genetic variation as  
277 in the stickleback, e.g. in East African cichlids<sup>9,75,76</sup>, in Darwin’s Finches<sup>69,77</sup> or in *Heliconius*  
278 butterflies<sup>78</sup>. Except for Darwin’s Finches<sup>79</sup> and our experiment however, it remains to be shown  
279 whether the colonization of new adaptive zones can occur similarly fast on contemporary time scales.  
280 Our findings suggests that multifarious divergent selection acts rapidly on many different genes and  
281 regions in the genome and that large steps in both phenotypic and genomic adaptation in adaptive

282 radiations are taken within the first few generations, even when starting from a highly derived  
283 adaptive radiation member. Adaptive radiations may thus rapidly advance on contemporary time  
284 scales, given enough standing genetic variation in key functional traits and an ecological theatre  
285 offering new niche space and imposing multifarious divergent selection.

286 **Methods**

287 **Experimental setup, sampling, ethics statement.** In May 1993, 100 adult giant threespine  
288 stickleback, 50 males and 50 females, were captured in Mayer Lake and transferred to Roadside Pond  
289 (aka ‘Mayer Pond’ in Leaver and Reimchen<sup>41</sup>). In 2004, 12 females were captured in Mayer Lake and  
290 in 2012, 11 females were caught in Roadside Pond corresponding to ~13 generations after release,  
291 assuming a population-average generation time of 1.5 years. In addition, stickleback from 25  
292 freshwater populations across the Haida Gwaii archipelago representing the range of successfully  
293 colonized freshwater habitats, were sampled between 1993 and 2012 (see Table 1 in Marques, et  
294 al.<sup>59</sup>). Stickleback were captured using minnow traps and euthanized with an overdose of tricaine  
295 methanesulfonate (MS-222) in agreement with British Columbia’s guidelines for scientific fish  
296 collection, under Ministry of Environment permits SM09-51584 and SM10-62059 and University of  
297 Victoria Aquatic Unit facility Standard Operating Procedure OA2003. Collections in Naikoon  
298 Provincial Park and Drizzle Lake Ecological Reserve were carried out under park use permits:  
299 103171, 103172, 104795 and 104796. Samples were stored in 70% ethanol and the genomes of 58  
300 individuals, including 12 Mayer Lake, 11 Roadside Pond and 1-4 individuals from 25 Haida Gwaii  
301 freshwater populations and two mainland British Columbia freshwater populations and one marine  
302 population were re-sequenced and are listed in Table 1 in our previous study focussing on the  
303 evolution of colour vision<sup>59</sup>. Alignment, variant and genotype calling and filtering is described in  
304 Marques, et al.<sup>59</sup>. Note that we aligned against an improved ordering of scaffolds of the reference  
305 stickleback genome and all genomic coordinates refer to this improved reference<sup>80</sup>. For the analyses in  
306 this study, we used either raw aligned reads with mapping quality  $\geq 17$  and bases with quality  $\geq 17$  for  
307 statistics computed on genotype likelihoods or one of two subsets from the SNP dataset containing  
308 7,888,602 high-quality SNPs among the 58 sequenced individuals for principal component analysis  
309 (unphased SNPs) and haplotype-based statistics (phased and imputed SNPs). The first, ‘selection  
310 experiment’ subset contained 4,180,622 SNPs among 12 Mayer Lake and 11 Roadside Pond  
311 individuals and the second ‘adaptive radiation’ dataset 6,564,510 SNPs among one marine and 25  
312 natural Haida Gwaii freshwater populations (including Mayer Lake) with one randomly picked  
313 individual per population. Read-backed phasing and imputation in both adaptive radiation and  
314 selection experiment SNP datasets was performed with SHAPEIT v2.r790<sup>81</sup>, with phase-informative  
315 reads covering on average 7.5% of all heterozygote genotypes and 30.9% of all graph segments.

316 **Population genomic analyses.** We described genomic change in the selection experiment with the  
317 statistics absolute allele frequency change ( $|\Delta AF|$ ), differentiation ( $F_{ST}$ ), nucleotide diversity ( $\pi$ ), and  
318 site frequency spectrum (Tajima’s D) computed from genotype likelihoods. We first computed the  
319 unfolded two-dimensional site frequency spectrum (2D-SFS) between Mayer Lake and Roadside  
320 Pond from aligned autosomal reads with angsd v0.915 and the reference genome as ancestral state.  
321 We used the 2D-SFS as prior to estimate  $F_{ST}$  at single sites as well as  $F_{ST}$ , Tajima’s D and  $\pi$  in  
322 windows of 10kb width, either non-overlapping or sliding with 2kb step size from raw aligned reads  
323 in angsd<sup>82-84</sup> with the filters as outlined above. Single site  $F_{ST}$  was calculated from site alphas and  
324 betas computed by angsd. We also estimated minor allele frequencies in each population in angsd to  
325 calculate absolute allele frequency change ( $|\Delta AF|$ ). We calculated a weighted mean  $|\Delta AF|$  with the  
326 weighted.mean function in R, using each SNP’s ‘starting allele frequency’, the minor allele frequency  
327 estimated for the Mayer Lake population, as weights.

328 We compared the amount of genomic change in the selection experiment to natural populations in the  
329 Haida Gwaii radiation for genome-wide differentiation ( $F_{ST}$ ) and absolute divergence ( $D_{XY}$ ). For

absolute divergence between the populations, we computed the unfolded 2D-SFS for pairs of individuals and calculated mean pairwise  $D_{XY}$  from the SFS using custom scripts. We computed pairwise  $D_{XY}$  within populations Mayer Lake and Roadside Pond to get a baseline of expected pairwise  $D_{XY}$ . Then we computed pairwise  $D_{XY}$  between populations Mayer Lake vs. Roadside Pond, three lake vs. stream ecotype populations (Mayer Lake vs. Gold Creek, Drizzle Lake vs. inlet and outlet, Spence Lake vs. outlet) and three large lake vs. small pond populations (Mayer Lake vs. Branta, Laurel, Solstice). We also estimated absolute divergence from the proportion of fixed differences among polymorphic sites between pairs of individuals. We annotated SNPs in the ‘adaptive radiation’ dataset using the Ensembl Variant Effect Predictor<sup>85</sup> and used the Picard Tool LiftOverVCF v2.7.0<sup>86</sup> to move the SNPs into the original annotation<sup>7</sup>. We partitioned SNPs into missense, synonymous, intron, regulatory and intergenic SNPs using SnpSift v4.2<sup>87</sup> and computed the proportion of fixed differences from the 012 output format of vcftools v0.1.15<sup>88</sup>. Genome-wide differentiation between populations ( $F_{ST}$ ) was calculated from previously published SNP array data<sup>34,46</sup> for the lake vs. stream and large lake vs. small pond comparisons. We ran a locus-by-locus AMOVA for SNPs with at least 3 genotypes per population in arlequin v3.5.2.2<sup>89</sup> (Supplementary Table 4), resulting in >400 SNPs per comparison that should give an unbiased genome-wide  $F_{ST}$  estimate<sup>90</sup>. For lake vs. stream comparisons with multiple stream populations (e.g. Drizzle: inlet and outlet; Mayer: Gold, Woodpile and Spam Creek<sup>46</sup>), we used hierarchical AMOVAs with each population retained as separate sample but grouped into either lake or stream group (Supplementary Table 4). Alpha and beta estimates from the AMOVA and the  $F_{ST}$  computation in angsd for Mayer vs. Roadside were pooled to sums of nominators and denominators to get a weighed mean  $F_{ST}$  estimate<sup>91</sup>.

We identified likely genomic targets of divergent selection between the source and transplant population with a two-step outlier approach. First, we inferred an optimal, neutral demographic model on the 2D-SFS using fastsimcoal2 v2.6<sup>92</sup>. Second, we simulated neutral genomic data under the best demographic model, against which we identified outlying genomic regions in the observed data. We folded the 2D-SFS using custom scripts, fit 12 different demographic models (Supplementary Fig. 2b and Data 1) to the observed 2D-SFS with fastsimcoal2 and compared their likelihoods using the Akaike information criterion (AIC) following Excoffier, et al.<sup>92</sup>. We maximized the likelihood of each model from 100 random starting parameter combinations in 10 to max. 50 ECM cycles, with a stopping criterion of 0.001. 100,000 coalescent simulations were used to approximate the expected 2D-SFS. In all simulations, we used a mutation rate of 1.7E-8, following Feulner, et al.<sup>93</sup>, a founding population size of 2N = 200 individuals for the Roadside Pond population and generated Mayer Lake samples 5 generations prior to Roadside Pond to account for different sampling years (Supplementary Data 1). Likelihood and parameter estimates for each model were obtained from the run with the highest likelihood among the 100 optimizations. For the parameters of the best model, we estimated 95%-confidence intervals as empirical percentiles on parameters from the best of 10 optimization runs on 100 bootstrap replicates of the observed 2D-SFS, with each optimization started from the original parameters of the best model. We computed bootstrap replicates for each autosome separately in angsd and combined 2D-SFS from different autosome with custom scripts. We simulated neutral genomic data under the best demographic model with fastsimcoal2 for four different recombination rates, high = 4-16 cM/Mb, intermediate = 1.5-4 cM/Mb, low = 0.5-1.5 cM/Mb and very low = 0-0.05 cM/Mb. For each recombination range, we generated 1,000 replicate DNA segments of 1Mb length, with a mutation rate of 1.7E-8 and a random recombination rate from that range, assuming a uniform distribution (very low, low recombination rate) or log-uniform distribution (intermediate, high recombination rate) that reflect the frequency of recombination rate variation in the stickleback genome<sup>80</sup>. We transformed the simulated data into VCF format using custom scripts and computed weighted  $F_{ST}$ , Tajima’s D and  $\pi$  in non-overlapping 10kb windows using vcftools v0.1.14<sup>88</sup>.

A selective sweep caused by divergent selection between habitats is expected to lead to excess differentiation ( $F_{ST}$ ) between populations at and around the site under selection, to reduced diversity in the population experiencing the selective sweep and to a shifted SFS, reflected by a strongly

negative Tajima's D upon completion of the sweep. In addition, haplotype-based statistics are able to detect soft and incomplete sweeps within a populations (iHS<sup>94</sup> and H12<sup>95</sup>) or completed sweeps in one of two populations (XPEHH)<sup>96</sup>. We computed the haplotype-based selection statistics integrated haplotype score (iHS)<sup>94</sup>, H12<sup>95</sup>, and cross-population extended haplotype homozygosity (XPEHH)<sup>96</sup> for phased and imputed bi-allelic SNPs with minor allele frequency > 5% in the 'selection experiment' dataset and for simulated SNP data. We computed iHS and H12 separately for Mayer Lake and Roadside Pond populations, using only SNPs with minor allele frequency > 5% in the respective population. We calculated the proportion of extreme iHS and XPEHH values ('w-iHS', the proportion of |iHS| > 2, following Voight, et al.<sup>94</sup> and 'w-XPEHH', the proportion of |XPEHH| > 2) in non-overlapping 10kb windows containing more than 10 iHS or XPEHH estimates, respectively, for both observed and simulated datasets. We used selscan v1.1.0b<sup>97</sup> with default parameters to compute iHS and XPEHH and the proportion of extreme values in 10kb windows. We also computed H12 for the observed dataset using scripts published alongside the H12 method<sup>95</sup>, with 81 SNPs bin width, resulting in on average 8.3kb wide windows close to the 10kb windows identified as optimal and robust to various demographic scenarios by Garud, et al.<sup>95</sup>.

We identified outliers against neutral expectations for six 10kb non-overlapping window statistics:  $F_{ST}$ , change in nucleotide diversity ( $\Delta\pi = \pi_{Roadside} - \pi_{Mayer}$ ), change in Tajima's D ( $\Delta T_D = T_{D,Roadside} - T_{D,Mayer}$ ), w-iHS<sub>Mayer</sub>, w-iHS<sub>Roadside</sub> and w-XPEHH. Our ability to detect signatures of selective sweeps with window-based statistics depends on local recombination rate, with stronger hitchhiking in low recombination rate regions leading to more prominent signals and a greater variation in such statistics (Supplementary Figs. 3-4). We therefore identified outlier windows separately in genomic regions with high, intermediate, low and very low recombination rate (see above and Supplementary Fig. 4). We assigned 10kb windows to recombination rate bins according to local recombination rates estimated in the middle of each 10kb window as described previously<sup>59</sup>. For each 10kb window, we computed the empirical quantile of the observed  $F_{ST}$ ,  $\Delta\pi$ ,  $\Delta T_D$ , w-iHS<sub>Mayer</sub>, w-iHS<sub>Roadside</sub> and w-XPEHH value against the simulated distribution of the statistic in the respective recombination bin with the function 'ecdf' in R v3.3.1<sup>98</sup>. We converted quantiles to two-sided p-values for  $\Delta\pi$  and  $\Delta T_D$  and one-sided p-values for the other statistics.

We identified genomic regions likely under divergent selection between Mayer Lake and Roadside Pond ('outlier regions') based on overlapping outlier signatures in these six selection statistics. To capture the shared signal, we applied Fisher's combined probability test to the four to six p-values in each 10kb window, as implemented in the R-package 'metap'. P-values from Fisher's combined probability test were corrected for multiple testing using the false discovery rate method<sup>99</sup> implemented in 'p.adjust', converted to q-values ( $= 1 - p_{adj}$ ) and z-transformed using the R function 'qnorm'. We used a Hidden Markov model (HMM) approach to group adjacent 10kb windows into outlier regions. The z-transformed q-values were used as input to HMMs with two or three normally distributed states. We optimized parameters of both HMMs from 1,000 random starting parameters using the Baum-Welch algorithm implemented in the R-package 'HiddenMarkov'. The three-state HMM better fit the data according to the Akaike information criterion and was thus used to assign all 42,996 10kb-windows to the three states using the Viterbi algorithm. Preliminary outlier regions were obtained from joining adjacent windows assigned to the state capturing highly significant Fisher's combined probability test p-values. Then, only outlier regions that contained significant outliers with  $p < 0.01$  for each of the statistics (a)  $F_{ST}$ , (b)  $\Delta\pi$  or  $\Delta T_D$  and (c) w-iHS<sub>Mayer</sub>, w-iHS<sub>Roadside</sub> or w-XPEHH as well as outlier regions with strongly aligned signatures for these statistics plus H12<sub>Mayer</sub> or H12<sub>Roadside</sub> were retained in the final set of outlier regions reflecting divergent selection between Mayer Lake and Roadside Pond. We did not further analyse signatures of e.g. shared directional or background selection, which should result in reduced diversity and Tajima's D or significant haplotype-based statistics in both populations, but not in differentiation between the populations.

We quantified adaptive differentiation between the source and transplant population by computing single SNP  $F_{ST}$  and retaining the top 5%  $F_{ST}$  SNPs in each outlier region, thereby containing likely the few SNPs under selection and many more linked, hitchhiking SNPs in each region affected by divergent selection. We compared this distribution of adaptive differentiation to adaptive differentiation among three postglacial pairs of lake and stream ecotypes on Haida Gwaii, using  $F_{ST}$  estimates from only those SNPs previously identified to be under selection in the respective ecotype comparison<sup>46</sup>, which also likely reflect SNPs hitchhiking and to a lesser degree direct targets of selection. For the top 5%  $F_{ST}$  SNPs in each outlier region, we computed the expected selection coefficient under a pure selection model, based on the allele frequency changes at these SNPs over 12.7 generations and assuming incomplete dominance  $h = 0.5$  following equation 3.2 in Gillespie<sup>100</sup>. These calculations likely overestimate selection coefficients due to unaccounted contributions of drift and should thus be interpreted with caution.

We computed linkage disequilibrium (LD) as  $r^2$  between the most divergent 15 SNPs polymorphic in both Mayer Lake and Roadside Pond for each outlier region using vcftools, both within and between chromosomes. We assessed whether LD between outlier regions on different chromosomes exceeded neutral expectations of no linkage disequilibrium. We derived the neutral distribution of LD with the observed sample sizes by randomly choosing SNPs outside outlier regions from each chromosome with at least 500kb distance between SNPs on the same chromosome ( $N = 617$ ) and computing inter-chromosomal LD between these SNPs. Then, we determined whether the mean observed LD between two outlier regions is greater than the 95%-quantile of the neutral observed inter-chromosomal LD distribution.

We associated the genomic signatures of divergent selection with potential sources of selection in the experiment and the adaptive radiation by studying their gene content and the gene's functional annotations, from their overlap with previously described stickleback QTL that have been mapped in genetic studies of specific phenotypes<sup>47</sup>, and from genotype-phenotype/ecology associations across the Haida Gwaii radiation. First, we identified candidate genes by inspecting the patterns of 10kb sliding window statistics  $F_{ST}$ ,  $\pi_{Mayer}$ ,  $\pi_{Roadside}$ , Tajima's D and single locus statistics  $iHS_{Mayer}$ ,  $iHS_{Roadside}$ ,  $H12_{Mayer}$ ,  $H12_{Roadside}$ , XPEHH and  $|\Delta AF|$  visually (Fig. 4, Supplementary Figs. 5-19) and retained a list of genes centred on or adjacent to selective sweep signatures (Supplementary Table 3). Then, we tested this list of candidate genes for enrichment of gene ontology terms using the String database v10<sup>101</sup> and retrieved functional and expression information from zebrafish<sup>58</sup> and related mouse, rat and human databases<sup>102,103</sup>. In addition, we identified overlap between outlier regions and QTL previously identified in other stickleback populations in the Northern Hemisphere using the list of Peichel and Marques<sup>47</sup> and the peak marker location and confidence intervals reported there. QTL were grouped into major, intermediate or minor effect size classes respectively, when they explained > 25%, between 5% and 25%, or < 5%, respectively, of the phenotypic variation in the experiments<sup>47</sup>.

Finally, we determined whether outlier regions in the selection experiment evolved in predictable directions given the environmental contrast. In the absence of replicate experimental ponds, we used genotype-phenotype and genotype-environment associations across the larger Haida Gwaii stickleback adaptive radiation with many natural replicates to infer whether the same genomic regions evolved in parallel direction. For each outlier region, we identified the SNPs with the strongest allele frequency change between Mayer Lake and Roadside Pond (top 1%  $|\Delta AF|$ ), assigned the alleles as Mayer Lake-like or Roadside Pond-like based on in which population they are more frequent, extracted the genotypes for those SNPs from the adaptive radiation SNP dataset containing single genomes of one marine and 25 freshwater populations including Mayer Lake, recoded the alleles as 0 (Mayer-like) or 1 (Roadside-like), combined them into multi-dimensional scaling (MDS) factors and polarized the MDS factors for Mayer Lake to be represented by low and Roadside Pond by high values in R. Next, we used the genomic MDS factor of each outlier region as response variable in a generalized linear model with 12 phenotypic and ecological properties of the 26 Haida Gwaii

477 populations as predictors (see below). For each outlier region's generalized linear model, we  
478 performed variable selection by iteratively removing non-significant predictors ( $\chi^2$  tests,  $P > 0.1$ ).  
479 Parallelism was inferred if the MDS factor of an outlier region was positively associated with the  
480 predictors, no parallelism if the association was negative.

481 We used the presence of blackwater (transmission at 400nm < 74%), of vertebrate predators in a  
482 population, and whether the population consists of predominantly melanistic phenotypes as binary  
483 predictors. Continuous predictors were lake area (log-transformed), light spectrum, mean body size  
484 (standard length), mean lateral plate number (excluding fully plated individuals), mean dorsal spine  
485 length, mean pelvic spine length, mean jaw length and mean gill raker number, the linear  
486 measurements size-corrected as described in Reimchen, et al.<sup>30</sup> and all scaled and standardized to  
487 mean zero and standard deviation one. We polarized all predictors so that the change from Mayer  
488 Lake to Roadside Pond would represent a positive shift, i.e. a shift from blackwater to clearwater,  
489 from melanism to reduced melanism, a decrease in lake area, body size, lateral plate number, pelvic  
490 spine length and gill raker number, and an increase in jaw length<sup>41</sup>. As last predictor, we included  
491 geographic structuring by using the first principal components axis from genomic variation in the  
492 adaptive radiation SNP dataset. We used genotype likelihoods from the adaptive radiation SNP  
493 dataset, computed the site allele frequency spectrum to get a covariance matrix as implemented in  
494 *angsd* and *ngsCovar*<sup>84</sup> and performed the eigenvalue decomposition in R to get the first principal  
495 component. We visualized phenotypic change in the selection experiment<sup>41</sup> and phenotypic  
496 divergence between Mayer Lake, it's stream ecotype (Mayer Stream = Gold Creek<sup>46</sup>), Laurel, Branta  
497 and Solstice<sup>39</sup> from the data of this earlier work by using the size-correction of Leaver and  
498 Reimchen<sup>41</sup> within each population for all datasets combined. Analyses were performed on Compute  
499 Canada's WestGrid computer cluster infrastructure ([www.westgrid.ca](http://www.westgrid.ca)).

500 **Data availability.** Aligned sequences can be accessed under accession SRP100209 on the NCBI short  
501 read archive ([www.ncbi.nlm.nih.gov/sra](http://www.ncbi.nlm.nih.gov/sra)).

502 **Code availability.** Custom scripts to compute  $D_{XY}$  from the SFS, to fold 2D-SFS and to fit HMM are  
503 available on <https://github.com/marqueda>.

#### 504 **Acknowledgments**

505 We thank Bruce Deagle, Stephen D. Leaver, Craig B. Lowe, Shannon D. Brady, Jason Turner, Kerstin  
506 Lindblad-Toh and the Broad Genomics Platforms for help with sequences, samples and morphometric  
507 analysis and Belaid Moa for bioinformatics support. This work was funded by the National Research  
508 Council Canada grant NRC2354 to T.E.R. and the National Institute of Health grants  
509 3P50HG002568-09S1 ARRA and 3P50HG002568 to D.M.K.

#### 510 **Author contributions**

511 T.E.R. conceived the study, ran the experiment, collected fish and ecological data in the field and  
512 acquired morphological data; D.M.K., F.C.J. and F.D.P. generated sequencing data and genotype  
513 calls, D.A.M. designed and performed all subsequent analyses and wrote the manuscript with  
514 contributions from all co-authors.

#### 515 **Competing interests**

516 The authors declare no competing financial interests.

517 Requests for materials should be addressed to T.E.R.

518 **References**

- 519 1 Schluter, D. *The ecology of adaptive radiation*. (Oxford University Press, 2000).  
520 2 Grant, P. R. Speciation and the Adaptive Radiation of Darwin Finches. *American Scientist* **69**,  
521 653-663, (1981).
- 522 3 Losos, J. B., Jackman, T. R., Larson, A., Queiroz, K. & Rodriguez-Schettino, L. Contingency  
523 and determinism in replicated adaptive radiations of island lizards. *Science* **279**, 2115-2118,  
524 (1998).
- 525 4 West-Eberhard, M. J. *Developmental plasticity and evolution*. (Oxford University Press,  
526 2003).
- 527 5 Muschick, M., Barluenga, M., Salzburger, W. & Meyer, A. Adaptive phenotypic plasticity in  
528 the Midas cichlid fish pharyngeal jaw and its relevance in adaptive radiation. *BMC Evol Biol*  
529 **11**, 116, (2011).
- 530 6 Barrett, R. D. & Schluter, D. Adaptation from standing genetic variation. *Trends Ecol Evol*  
531 **23**, 38-44, (2008).
- 532 7 Jones, F. C. *et al.* The genomic basis of adaptive evolution in threespine sticklebacks. *Nature*  
533 **484**, 55-61, (2012).
- 534 8 Seehausen, O. Hybridization and adaptive radiation. *Trends Ecol Evol* **19**, 198-207, (2004).
- 535 9 Meier, J. I. *et al.* Ancient hybridization fuels rapid cichlid fish adaptive radiations. *Nat  
536 Commun* **8**, 14363, (2017).
- 537 10 Price, T. D., Qvarnstrom, A. & Irwin, D. E. The role of phenotypic plasticity in driving  
538 genetic evolution. *Proc Biol Sci* **270**, 1433-1440, (2003).
- 539 11 Schlotterer, C., Kofler, R., Versace, E., Tobler, R. & Franssen, S. U. Combining experimental  
540 evolution with next-generation sequencing: a powerful tool to study adaptation from standing  
541 genetic variation. *Heredity (Edinb)* **116**, 248, (2016).
- 542 12 Barrett, S. C. H., I., C. R., Dlugosch, K. M. & Rieseberg, L. H. *Invasion Genetics: The Baker  
543 and Stebbins Legacy*. (Wiley-Blackwell, 2016).
- 544 13 Burke, M. K. *et al.* Genome-wide analysis of a long-term evolution experiment with  
545 *Drosophila*. *Nature* **467**, 587-590, (2010).
- 546 14 Fritz, M. L. *et al.* Contemporary evolution of a Lepidopteran species, *Heliothis virescens*, in  
547 response to modern agricultural practices. *Mol Ecol* **27**, 167-181, (2018).
- 548 15 Tobler, R. *et al.* Massive habitat-specific genomic response in *D. melanogaster* populations  
549 during experimental evolution in hot and cold environments. *Mol Biol Evol* **31**, 364-375,  
550 (2014).
- 551 16 Graves, J. L., Jr. *et al.* Genomics of parallel experimental evolution in *Drosophila*. *Mol Biol  
552 Evol*, (2017).
- 553 17 Huang, Y., Wright, S. I. & Agrawal, A. F. Genome-wide patterns of genetic variation within  
554 and among alternative selective regimes. *PLoS Genet* **10**, e1004527, (2014).
- 555 18 Franks, S. J., Kane, N. C., O'Hara, N. B., Tittes, S. & Rest, J. S. Rapid genome-wide  
556 evolution in *Brassica rapa* populations following drought revealed by sequencing of ancestral  
557 and descendant gene pools. *Mol Ecol* **25**, 3622-3631, (2016).
- 558 19 van't Hof, A. E., Edmonds, N., Dalikova, M., Marec, F. & Saccheri, I. J. Industrial melanism  
559 in British peppered moths has a singular and recent mutational origin. *Science* **332**, 958-960,  
560 (2011).
- 561 20 Reid, N. M. *et al.* The genomic landscape of rapid repeated evolutionary adaptation to toxic  
562 pollution in wild fish. *Science* **354**, 1305-1308, (2016).
- 563 21 Fraser, B. A., Kunstner, A., Reznick, D. N., Dreyer, C. & Weigel, D. Population genomics of  
564 natural and experimental populations of guppies (*Poecilia reticulata*). *Mol Ecol* **24**, 389-408,  
565 (2015).
- 566 22 Hendry, A. P. & Kinnison, M. T. Perspective: The pace of modern life: Measuring rates of  
567 contemporary microevolution. *Evolution* **53**, 1637-1653, (1999).
- 568 23 Reznick, D. N. & Ghalambor, C. K. The population ecology of contemporary adaptations:  
569 what empirical studies reveal about the conditions that promote adaptive evolution. *Genetica*  
570 **112-113**, 183-198, (2001).

- 571 24 Stockwell, C. A., Hendry, A. P. & Kinnison, M. T. Contemporary evolution meets  
572 conservation biology. *Trends Ecol Evol* **18**, 94-101, (2003).
- 573 25 Bell, M. A., Aguirre, W. E. & Buck, N. J. Twelve years of contemporary armor evolution in a  
574 threespine stickleback population. *Evolution* **58**, 814-824, (2004).
- 575 26 Terekhanova, N. V. *et al.* Fast evolution from precast bricks: genomics of young freshwater  
576 populations of threespine stickleback *Gasterosteus aculeatus*. *PLoS Genet* **10**, e1004696,  
577 (2014).
- 578 27 Lescak, E. A. *et al.* Evolution of stickleback in 50 years on earthquake-uplifted islands. *Proc  
579 Natl Acad Sci U S A* **112**, E7204-7212, (2015).
- 580 28 Aguirre, W. E. & Bell, M. A. Twenty years of body shape evolution in a threespine  
581 stickleback population adapting to a lake environment. *Biol J Linn Soc* **105**, 817-831, (2012).
- 582 29 Hohenlohe, P. A. *et al.* Population genomics of parallel adaptation in threespine stickleback  
583 using sequenced RAD tags. *PLoS Genet* **6**, e1000862, (2010).
- 584 30 Reimchen, T. E., Bergstrom, C. & Nosil, P. Natural selection and the adaptive radiation of  
585 Haida Gwaii stickleback. *Evol Ecol Res* **15**, 241-269, (2013).
- 586 31 Moodie, G. E. E. & Reimchen, T. E. Phenetic variation and habitat differences in  
587 *Gasterosteus* populations of Queen Charlotte Islands. *Syst Zool* **25**, 49-61, (1976).
- 588 32 Reimchen, T. E. & Douglas, S. Differential contribution of the sexes to prefledged young in  
589 red-throated loons. *Auk* **102**, 198-201, (1985).
- 590 33 Bergstrom, C. A. & Reimchen, T. E. Habitat dependent associations between parasitism and  
591 fluctuating asymmetry among endemic stickleback populations. *J Evol Biol* **18**, 939-948,  
592 (2005).
- 593 34 Deagle, B. E., Jones, F. C., Absher, D. M., Kingsley, D. M. & Reimchen, T. E.  
594 Phylogeography and adaptation genetics of stickleback from the Haida Gwaii archipelago  
595 revealed using genome-wide single nucleotide polymorphism genotyping. *Mol Ecol* **22**, 1917-  
596 1932, (2013).
- 597 35 Reimchen, T. E. Predator handling failures of lateral plate morphs in *Gasterosteus aculeatus*:  
598 Functional implications for the ancestral plate condition. *Behaviour* **137**, 1081-1096, (2000).
- 599 36 Reimchen, T. E. Spine deficiency and polymorphism in a population of *Gasterosteus  
600 aculeatus* - an adaptation to predators. *Can J Zool* **58**, 1232-1244, (1980).
- 601 37 Reimchen, T. E. & Nosil, P. Temporal variation in divergent selection on spine number in  
602 threespine stickleback. *Evolution* **56**, 2472-2483, (2002).
- 603 38 Reimchen, T. E. & Nosil, P. Variable predation regimes predict the evolution of sexual  
604 dimorphism in a population of threespine stickleback. *Evolution* **58**, 1274-1281, (2004).
- 605 39 Reimchen, T. E., Stinson, E. M. & Nelson, J. S. Multivariate differentiation of parapatric and  
606 allopatric populations of threespine stickleback in the Sangan river watershed, Queen-  
607 Charlotte islands. *Can J Zool* **63**, 2944-2951, (1985).
- 608 40 Spoljaric, M. A. & Reimchen, T. E. 10 000 years later: evolution of body shape in Haida  
609 Gwaii three-spined stickleback. *J Fish Biol* **70**, 1484-1503, (2007).
- 610 41 Leaver, S. D. & Reimchen, T. E. Abrupt changes in defence and trophic morphology of the  
611 giant threespine stickleback (*Gasterosteus* sp.) following colonization of a vacant habitat. *Biol  
612 J Linn Soc* **107**, 494-509, (2012).
- 613 42 Moodie, G. E. E. Morphology, life-History, and ecology of an unusual stickleback  
614 (*Gasterosteus aculeatus*) in Queen-Charlotte Islands, Canada. *Can J Zool* **50**, 721-732,  
615 (1972).
- 616 43 Moodie, G. E. E. Predation, natural selection and adaptation in an unusual threespine  
617 stickleback. *Heredity* **28**, 155-167, (1972).
- 618 44 O'Reilly, P., Reimchen, T. E., Beech, R. & Strobeck, C. Mitochondrial-DNA in *Gasterosteus*  
619 and pleistocene glacial refugium on the Queen-Charlotte-Islands, British-Columbia. *Evolution*  
620 **47**, 678-684, (1993).
- 621 45 Flamarique, I. N., Bergstrom, C., Cheng, C. L. & Reimchen, T. E. Role of the iridescent eye  
622 in stickleback female mate choice. *J Exp Biol* **216**, 2806-2812, (2013).
- 623 46 Deagle, B. E. *et al.* Population genomics of parallel phenotypic evolution in stickleback  
624 across stream-lake ecological transitions. *Proc Biol Sci* **279**, 1277-1286, (2012).

- 625 47 Peichel, C. L. & Marques, D. A. The genetic and molecular architecture of phenotypic  
626 diversity in sticklebacks. *Philos Trans R Soc Lond B Biol Sci* **372**, (2017).
- 627 48 Peichel, C. L. *et al.* The genetic architecture of divergence between threespine stickleback  
628 species. *Nature* **414**, 901-905, (2001).
- 629 49 Colosimo, P. F. *et al.* Widespread parallel evolution in sticklebacks by repeated fixation of  
630 Ectodysplasin alleles. *Science* **307**, 1928-1933, (2005).
- 631 50 Colosimo, P. F. *et al.* The genetic architecture of parallel armor plate reduction in threespine  
632 sticklebacks. *PLoS Biol* **2**, E109, (2004).
- 633 51 Wark, A. R. *et al.* Genetic architecture of variation in the lateral line sensory system of  
634 threespine sticklebacks. *G3* **2**, 1047-1056, (2012).
- 635 52 Greenwood, A. K., Wark, A. R., Yoshida, K. & Peichel, C. L. Genetic and neural modularity  
636 underlie the evolution of schooling behavior in threespine sticklebacks. *Curr Biol* **23**, 1884-  
637 1888, (2013).
- 638 53 Rennison, D. J., Owens, G. L., Heckman, N., Schluter, D. & Veen, T. Rapid adaptive  
639 evolution of colour vision in the threespine stickleback radiation. *Proc Biol Sci* **283**,  
640 20160242, (2016).
- 641 54 Perez-Leighton, C. E., Schmidt, T. M., Abramowitz, J., Birnbaumer, L. & Kofuji, P. Intrinsic  
642 phototransduction persists in melanopsin-expressing ganglion cells lacking diacylglycerol-  
643 sensitive TRPC subunits. *Eur J Neurosci* **33**, 856-867, (2011).
- 644 55 Nakajima, Y., Moriyama, M., Hattori, M., Minato, N. & Nakanishi, S. Isolation of ON bipolar  
645 cell genes via hrGFP-coupled cell enrichment using the mGluR6 promoter. *J Biochem* **145**,  
646 811-818, (2009).
- 647 56 Amsterdam, A. *et al.* Identification of 315 genes essential for early zebrafish development.  
648 *Proc Natl Acad Sci U S A* **101**, 12792-12797, (2004).
- 649 57 Nuckels, R. J., Ng, A., Darland, T. & Gross, J. M. The vacuolar-ATPase complex regulates  
650 retinoblast proliferation and survival, photoreceptor morphogenesis, and pigmentation in the  
651 zebrafish eye. *Investigative ophthalmology & visual science* **50**, 893-905, (2009).
- 652 58 Howe, D. G. *et al.* ZFIN, the zebrafish model organism database: increased support for  
653 mutants and transgenics. *Nucleic acids research* **41**, D854-860, (2013).
- 654 59 Marques, D. A. *et al.* Convergent evolution of SWS2 opsin facilitates adaptive radiation of  
655 threespine stickleback into different light environments. *PLoS Biol* **15**, e2001627, (2017).
- 656 60 Gwynn, B., Smith, R. S., Rowe, L. B., Taylor, B. A. & Peters, L. L. A mouse TRAPP-related  
657 protein is involved in pigmentation. *Genomics* **88**, 196-203, (2006).
- 658 61 Hoekstra, H. E., Hirschmann, R. J., Bundey, R. A., Insel, P. A. & Crossland, J. P. A single  
659 amino acid mutation contributes to adaptive beach mouse color pattern. *Science* **313**, 101-104,  
660 (2006).
- 661 62 Dickinson, M. E. *et al.* High-throughput discovery of novel developmental phenotypes.  
662 *Nature* **537**, 508-514, (2016).
- 663 63 Ignatius, M. S., Moose, H. E., El-Hodiri, H. M. & Henion, P. D. colgate/hdac1 repression of  
664 foxd3 expression is required to permit mitfa-dependent melanogenesis. *Dev Biol* **313**, 568-  
665 583, (2008).
- 666 64 Patterson, L. B. & Parichy, D. M. Interactions with iridophores and the tissue environment  
667 required for patterning melanophores and xanthophores during zebrafish adult pigment stripe  
668 formation. *PLoS Genet* **9**, e1003561, (2013).
- 669 65 Miller, C. T. *et al.* cis-Regulatory changes in Kit ligand expression and parallel evolution of  
670 pigmentation in sticklebacks and humans. *Cell* **131**, 1179-1189, (2007).
- 671 66 Rosenblum, E. B., Hoekstra, H. E. & Nachman, M. W. Adaptive reptile color variation and  
672 the evolution of the *Mcl1r* gene. *Evolution* **58**, 1794-1808, (2004).
- 673 67 Malek, T. B., Boughman, J. W., Dworkin, I. & Peichel, C. L. Admixture mapping of male  
674 nuptial colour and body shape in a recently formed hybrid population of threespine  
675 stickleback. *Mol Ecol* **21**, 5265-5279, (2012).
- 676 68 Miller, C. T. *et al.* Modular skeletal evolution in sticklebacks is controlled by additive and  
677 clustered quantitative trait Loci. *Genetics* **197**, 405-420, (2014).
- 678 69 Lamichhaney, S. *et al.* A beak size locus in Darwin's finches facilitated character  
679 displacement during a drought. *Science* **352**, 470-474, (2016).

- 680 70 Gingerich, P. D. Rates of evolution: effects of time and temporal scaling. *Science* **222**, 159-  
681 161, (1983).
- 682 71 Rennison, D. J., Owens, G. L. & Taylor, J. S. Opsin gene duplication and divergence in ray-  
683 finned fish. *Mol Phylogenet Evol* **62**, 986-1008, (2012).
- 684 72 Reimchen, T. E. Predator-induced cyclical changes in lateral plate frequencies of  
685 *Gasterosteus*. *Behaviour* **132**, 1079-1094, (1995).
- 686 73 Stinson, E. M. *Threespine sticklebacks (Gasterosteus aculeatus) in Drizzle lake and its inlet,  
687 Queen Charlotte islands: ecological and behavioural relationships and their relevance to  
688 reproductive isolation* MSc thesis, University of Alberta, (1983).
- 689 74 Dlugosch, K. M. & Parker, I. M. Founding events in species invasions: genetic variation,  
690 adaptive evolution, and the role of multiple introductions. *Mol Ecol* **17**, 431-449, (2008).
- 691 75 Keller, I. *et al.* Population genomic signatures of divergent adaptation, gene flow and hybrid  
692 speciation in the rapid radiation of Lake Victoria cichlid fishes. *Mol Ecol* **22**, 2848-2863,  
693 (2013).
- 694 76 McGee, M. D., Neches, R. Y. & Seehausen, O. Evaluating genomic divergence and  
695 parallelism in replicate ecomorphs from young and old cichlid adaptive radiations. *Mol Ecol*  
696 **25**, 260-268, (2016).
- 697 77 Lamichhaney, S. *et al.* Evolution of Darwin's finches and their beaks revealed by genome  
698 sequencing. *Nature* **518**, 371-375, (2015).
- 699 78 Dasmahapatra, K. K. *et al.* Butterfly genome reveals promiscuous exchange of mimicry  
700 adaptations among species. *Nature* **487**, 94-98, (2012).
- 701 79 Grant, P. R. & Grant, B. R. Unpredictable evolution in a 30-year study of Darwin's finches.  
702 *Science* **296**, 707-711, (2002).
- 703 80 Glazer, A. M., Killingbeck, E. E., Mitros, T., Rokhsar, D. S. & Miller, C. T. Genome  
704 assembly improvement and mapping convergently evolved skeletal traits in sticklebacks with  
705 genotyping-by-sequencing. *G3* **5**, 1463-1472, (2015).
- 706 81 Delaneau, O., Howie, B., Cox, A. J., Zagury, J. F. & Marchini, J. Haplotype estimation using  
707 sequencing reads. *Am J Hum Genet* **93**, 687-696, (2013).
- 708 82 Korneliussen, T. S., Albrechtsen, A. & Nielsen, R. ANGSD: Analysis of Next Generation  
709 Sequencing Data. *BMC Bioinformatics* **15**, 356, (2014).
- 710 83 Nielsen, R., Korneliussen, T., Albrechtsen, A., Li, Y. & Wang, J. SNP calling, genotype  
711 calling, and sample allele frequency estimation from New-Generation Sequencing data. *PLoS  
712 One* **7**, e37558, (2012).
- 713 84 Fumagalli, M. *et al.* Quantifying population genetic differentiation from next-generation  
714 sequencing data. *Genetics* **195**, 979-992, (2013).
- 715 85 McLaren, W. *et al.* The Ensembl Variant Effect Predictor. *Genome Biol* **17**, 122, (2016).
- 716 86 Broad Institute. *Picard Tools*, <http://broadinstitute.github.io/picard> (accessed 30 January  
717 2017).
- 718 87 Cingolani, P. *et al.* A program for annotating and predicting the effects of single nucleotide  
719 polymorphisms, SnpEff: SNPs in the genome of *Drosophila melanogaster* strain w1118; iso-  
720 2; iso-3. *Fly (Austin)* **6**, 80-92, (2012).
- 721 88 Danecek, P. *et al.* The variant call format and VCFtools. *Bioinformatics* **27**, 2156-2158,  
722 (2011).
- 723 89 Excoffier, L. & Lischer, H. E. Arlequin suite ver 3.5: a new series of programs to perform  
724 population genetics analyses under Linux and Windows. *Mol Ecol Resour* **10**, 564-567,  
725 (2010).
- 726 90 Willing, E. M., Dreyer, C. & van Oosterhout, C. Estimates of genetic differentiation measured  
727 by F(ST) do not necessarily require large sample sizes when using many SNP markers. *PLoS  
728 One* **7**, e42649, (2012).
- 729 91 Bhatia, G., Patterson, N., Sankararaman, S. & Price, A. L. Estimating and interpreting FST:  
730 The impact of rare variants. *Genome Res* **23**, 1514-1521, (2013).
- 731 92 Excoffier, L., Dupanloup, I., Huerta-Sanchez, E., Sousa, V. C. & Foll, M. Robust  
732 demographic inference from genomic and SNP data. *PLoS Genet* **9**, e1003905, (2013).
- 733 93 Feulner, P. G. *et al.* Genomics of divergence along a continuum of parapatric population  
734 differentiation. *PLoS Genet* **11**, e1004966, (2015).

- 735 94 Voight, B. F., Kudaravalli, S., Wen, X. & Pritchard, J. K. A map of recent positive selection  
736 in the human genome. *PLoS Biol* **4**, e72, (2006).
- 737 95 Garud, N. R., Messer, P. W., Buzbas, E. O. & Petrov, D. A. Recent selective sweeps in North  
738 American *Drosophila melanogaster* show signatures of soft sweeps. *PLoS Genet* **11**,  
739 e1005004, (2015).
- 740 96 Sabeti, P. C. *et al.* Genome-wide detection and characterization of positive selection in human  
741 populations. *Nature* **449**, 913-U912, (2007).
- 742 97 Szpiech, Z. A. & Hernandez, R. D. selscan: an efficient multithreaded program to perform  
743 EHH-based scans for positive selection. *Mol Biol Evol* **31**, 2824-2827, (2014).
- 744 98 R Development Core Team. *R: A language and environment for statistical computing.*,  
745 <http://www.r-project.org/> (accessed 20 April 2016).
- 746 99 Benjamini, Y. & Hochberg, Y. Controlling the False Discovery Rate - a Practical and  
747 Powerful Approach to Multiple Testing. *Journal of the Royal Statistical Society Series B-*  
748 *Methodological* **57**, 289-300, (1995).
- 749 100 Gillespie, J. H. *Population genetics: a concise guide*. 2nd edn, (Johns Hopkins University  
750 Press, 2004).
- 751 101 Szklarczyk, D. *et al.* STRING v10: protein-protein interaction networks, integrated over the  
752 tree of life. *Nucleic acids research* **43**, D447-452, (2015).
- 753 102 Blake, J. A. *et al.* Mouse Genome Database (MGD)-2017: community knowledge resource  
754 for the laboratory mouse. *Nucleic acids research* **45**, D723-D729, (2017).
- 755 103 Shimoyama, M. *et al.* The Rat Genome Database 2015: genomic, phenotypic and  
756 environmental variations and disease. *Nucleic acids research* **43**, D743-750, (2015).

759 **Figure legends**

760 **Fig. 1 | Phenotypic and genomic change in the selection experiment.** **a** Summary of the phenotypic change  
 761 observed in the selection experiment, as reported in Leaver and Reimchen<sup>41</sup>, with colours indicating trait  
 762 increase or decrease and asterisks indicating significant change. Phenotypic change in six bony predator defence  
 763 traits (FSL: first dorsal spine length, SSL: second dorsal spine length, PSL: pelvic spine length, # plates: number  
 764 of lateral plates, LP3H: lateral plate 3 height, LP2: lateral plate 2 frequency), four feeding morphology traits  
 765 (LJL: lower jaw length, # rakers: number of gill rakers, GRL: gill raker length, GRS: gill raker spacing) and eye  
 766 diameter (ED) was in the expected direction, i.e. parallel, given the shift from vertebrate- to invertebrate-  
 767 dominated predation and zooplankton- to invertebrate-dominated diet and observed phenotypic divergence  
 768 between large lake and small pond populations in the adaptive radiation on Haida Gwaii<sup>41</sup>. SL: standard length.  
 769 **b** Transplant of 100 adult giant threespine stickleback from Mayer Lake into Roadside Pond and evolution for  
 770 13 generations led to moderate genomic differentiation ( $F_{ST}$ ), a minor reduction nucleotide diversity ( $\pi$ ) and to a  
 771 positive shift in the Tajima's D ( $T_D$ ) distribution. **c** Even though several rare alleles were fixed, allele  
 772 frequencies (AF) did not change much over 13 generations. MAF: minor allele frequency.

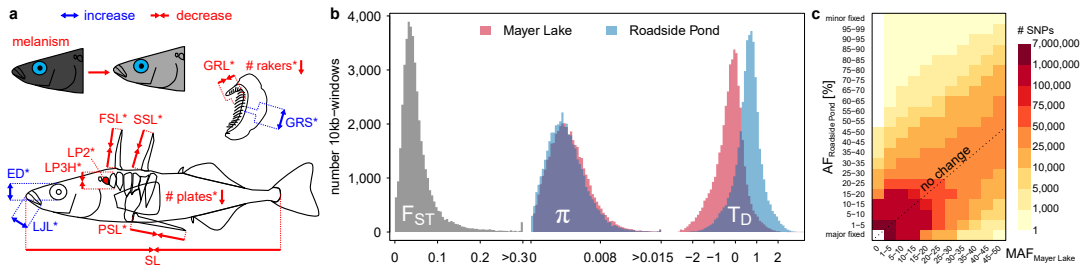
773 **Fig. 2 | Comparison of the extent of phenotypic and genomic evolution in the 19 years selection**  
 774 **experiment with the ~12,000 years old adaptive radiation.** Phenotypic divergence and adaptive genomic  
 775 differentiation arose rapidly in the selection experiment, comparable in extent to postglacial divergence between  
 776 large lake and pond or stream ecotypes. **a** Population means and distributions for six phenotypic traits in Mayer  
 777 Lake (source population), Roadside Pond (transplant population, orange), postglacial stream (green) and pond  
 778 (blue) ecotype populations<sup>41</sup>. **b** Absolute divergence ( $D_{XY}$ ), **c** relative differentiation ( $F_{ST}$ ) and **d** adaptive  
 779 differentiation ( $F_{ST}$ ) between postglacial large lake and stream (green) or pond (blue) ecotype populations as  
 780 well as in the selection experiment (orange).  $F_{ST}$  estimates for lake-stream and large lake vs. small pond  
 781 comparisons are based on SNP chip data from a previous study<sup>46</sup>. Adaptive differentiation SNPs are outlier  
 782 SNPs in this previous study<sup>46</sup> and top 5%  $F_{ST}$  SNPs in each outlier window for the selection experiment.  
 783 Numbers are mean percentages of phenotypic or genomic change in the selection experiment compared to  
 784 postglacial lake vs. stream divergence (upper) and large lake vs. small pond divergence (lower number).

785 **Fig. 3 | Genomic footprints of divergent selection are widespread across the genome.** **a** Absolute allele  
 786 frequency change ( $|\Delta AF|$ ) at the top 0.1% strongest  $|\Delta AF|$ -SNPs, with black points highlighting SNPs for which  
 787 the rarer allele in Mayer Lake went to fixation in Roadside Pond. Grey vertical bars highlight 77 outlier regions  
 788 across 15 of the 21 stickleback chromosomes (roman numerals) with overlapping top 1% outlier 10kb windows  
 789 against neutral demographic expectations highlighted with larger, darker points, for the statistics **b** high  
 790 differentiation ( $F_{ST}$ ), **c** change in diversity ( $\Delta \pi$ ) and **d** Tajima's D ( $\Delta T_D$ ) and haplotype-based selection statistics  
 791 **e** w-iHS and **f** w-XPEHH (see Methods).

792 **Fig. 4 | Local signatures of divergent selection in the genome.** For five of the 77 outlier regions in the genome  
 793 (grey shading), patterns of differentiation ( $F_{ST}$ ), allele frequency change ( $|\Delta AF|$ ), nucleotide diversity ( $\pi$ ),  
 794 Tajima's D ( $T_D$ ) and iHS, H12 and XPEHH are shown. Outlier region I.b is centred on a two genes, *trappc6bl*  
 795 and *bloc1s3*, controlling pigmentation in the retina, II.a contains the pigmentation gene *mc1r*, XVII.j the blue-  
 796 sensitive colour vision gene *opnsw2*, likely targets of divergent selection on pigmentation and visual perception.  
 797 See Supplementary Figs. 5-19 for further outlier regions. The top panel colour code indicates quantiles in the  
 798  $|\Delta AF|$  distribution, black horizontal bars show significant non-overlapping 10kb outlier windows against neutral  
 799 expectations, gene exons are shown on top (gene names 'ENSG0000000012345' shortened to 'e12345').  
 800 Genomic coordinates refer to an improved version of the reference genome<sup>80</sup>. Lines are sliding-window  
 801 estimates for 10kb sliding windows with 2.5kb step size, dots are single SNP estimates ( $|\Delta AF|$ , iHS, XPEHH) or  
 802 81-SNP windows (H12).

803 **Fig. 5 | Outlier regions and overlapping QTL, candidate genes and genome-phenotype/ecology**  
 804 **associations across the adaptive radiation.** **a** Distribution of overlapping quantitative trait loci (QTL). Circles  
 805 indicate QTL peak markers, horizontal bars confidence intervals and colour codes the effect sizes: major  
 806 (percentage variance explained, PVE > 25%), intermediate (25% > PVE > 5%) and minor effect QTL (PVE <  
 807 5%). **b** Genome vs. environment and phenotype associations (GE/GP assoc.) and directionality of phenotypic  
 808 and genomic change between selection experiment and Haida Gwaii adaptive radiation. Predictors retained in  
 809 generalized linear model for each outlier region are shown in coloured squares, with blue boxes representing  
 810 parallel genomic and phenotypic / ecological change and red boxes non-parallel change (except for genomic  
 811 PC1, for which directionality cannot be inferred). The colour code shows the relative effect sizes ( $\beta$ ). **c** List of  
 812 candidate genes centred on divergent selection patterns in outlier regions.

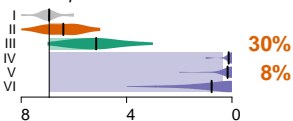




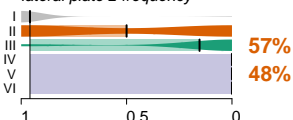
## Phenotypic Change

**a**

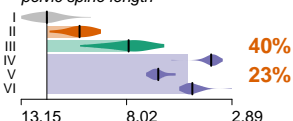
*lateral plate number*



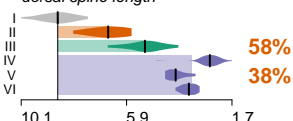
*lateral plate 2 frequency*



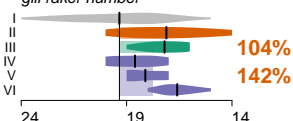
*pelvic spine length*



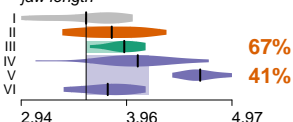
*dorsal spine length*



*gill raker number*



*jaw length*

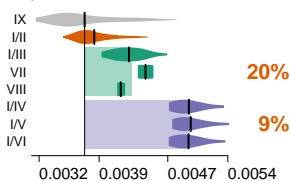


## Genomic Change

**b**

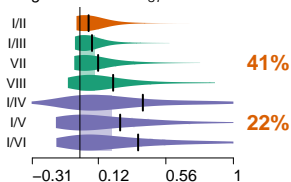
absolute divergence

pairwise  $D_{XY}$



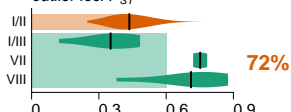
## c relative differentiation

genome-wide  $F_{ST}$

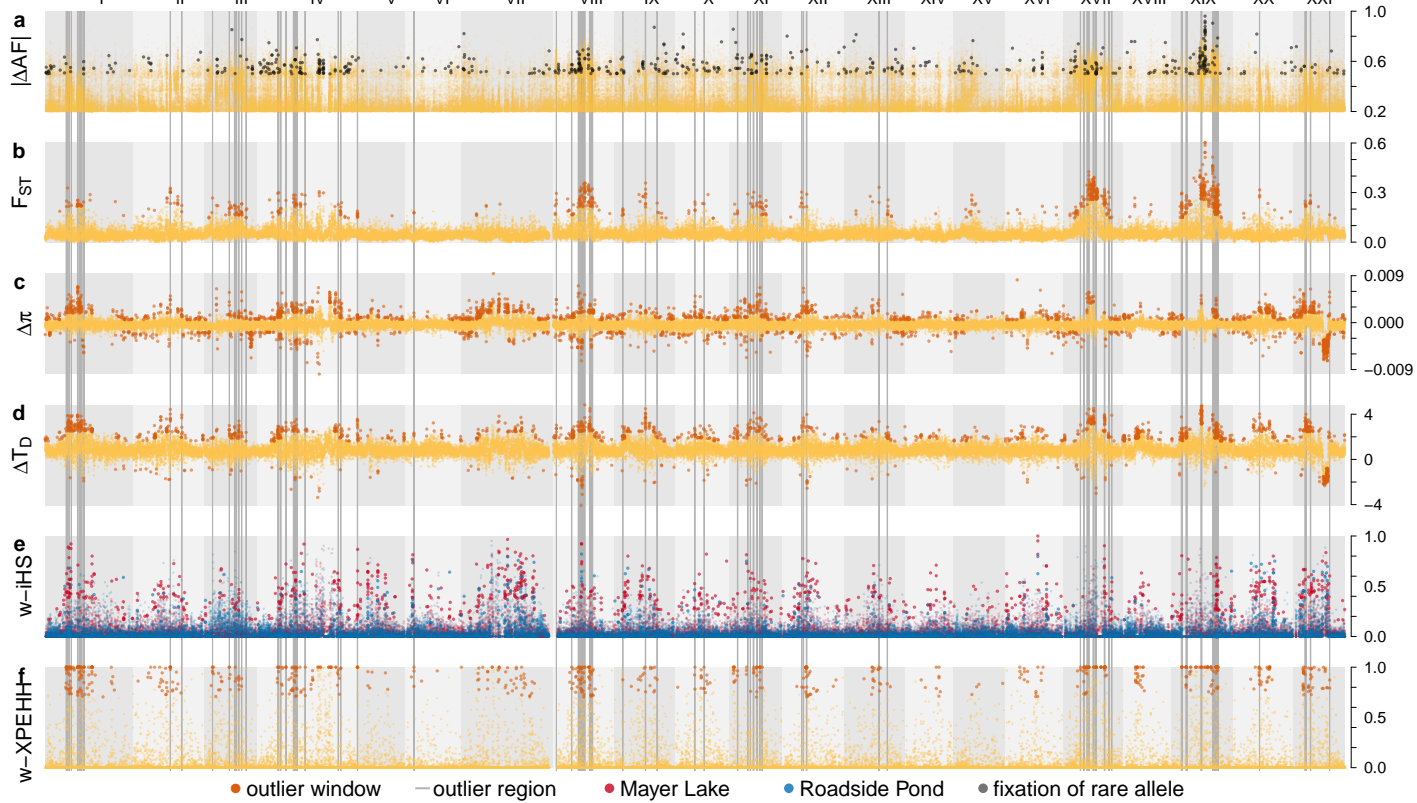


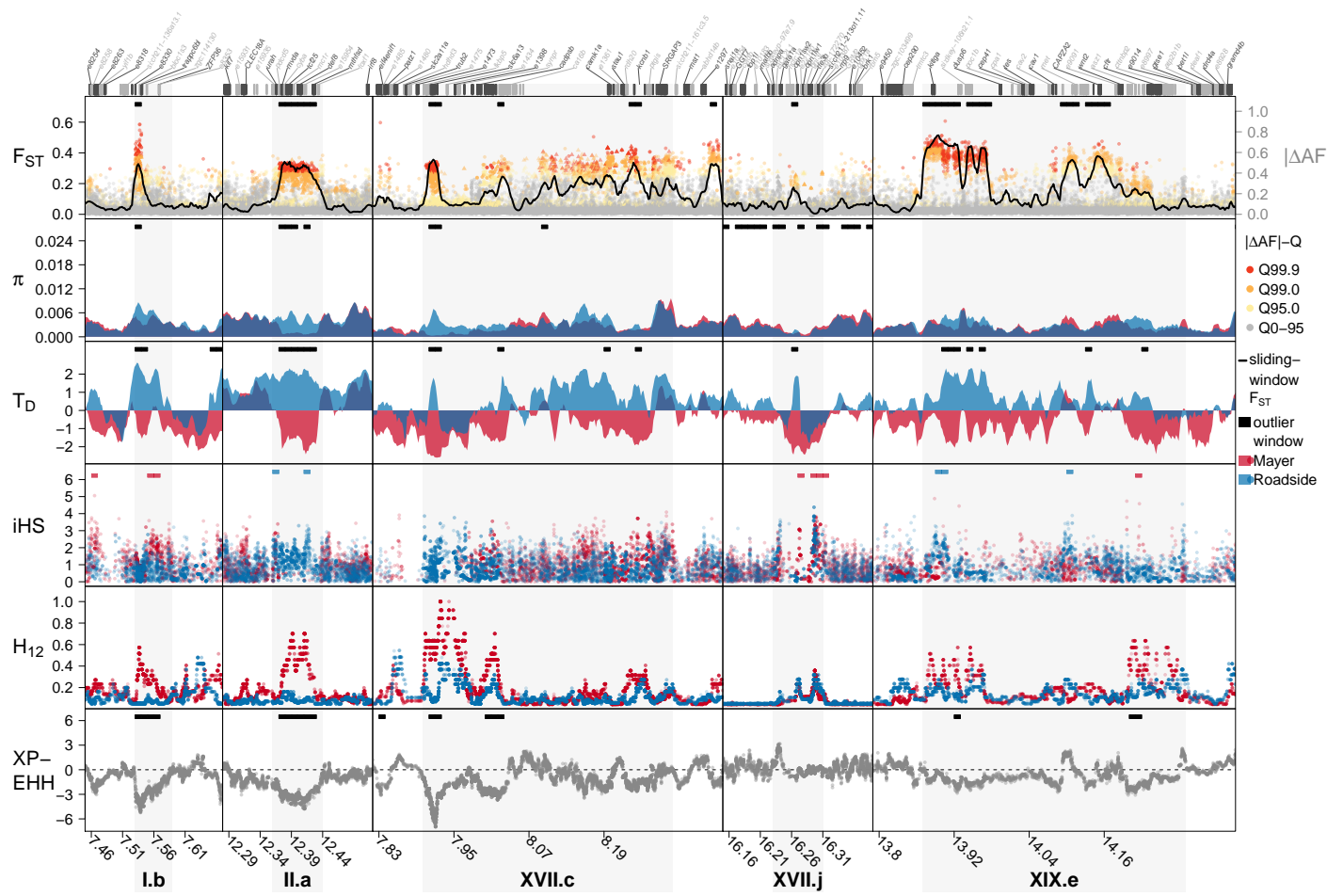
## d adaptive differentiation

outlier loci  $F_{ST}$



- Selection experiment
- Stream population/comparison
- Pond population/comparison
- Mayer Lake
- Roadside Pond
- Mayer Stream
- Branta Pond
- Laurel Pond
- Solstice Pond
- Spence Lake vs. Stream
- Drizzle Lake vs. Stream
- Mayer/Roadside within population





**a**

overlapping QTL

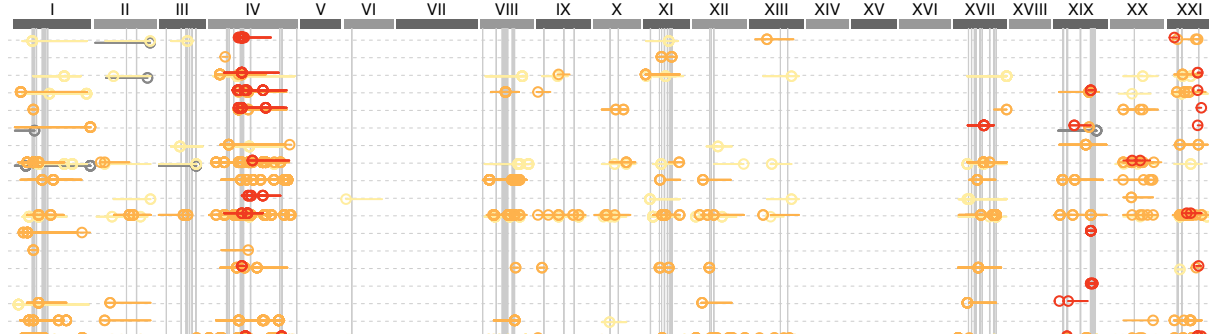
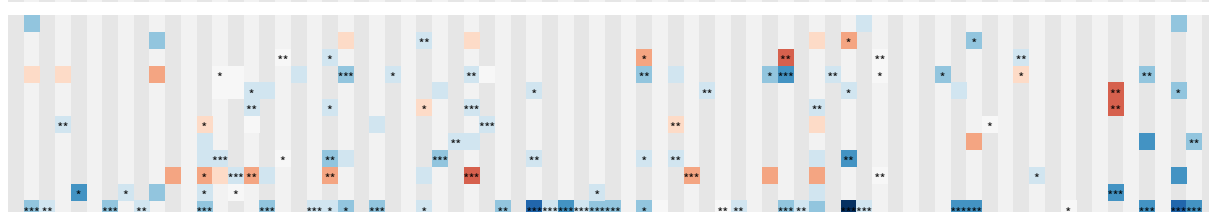


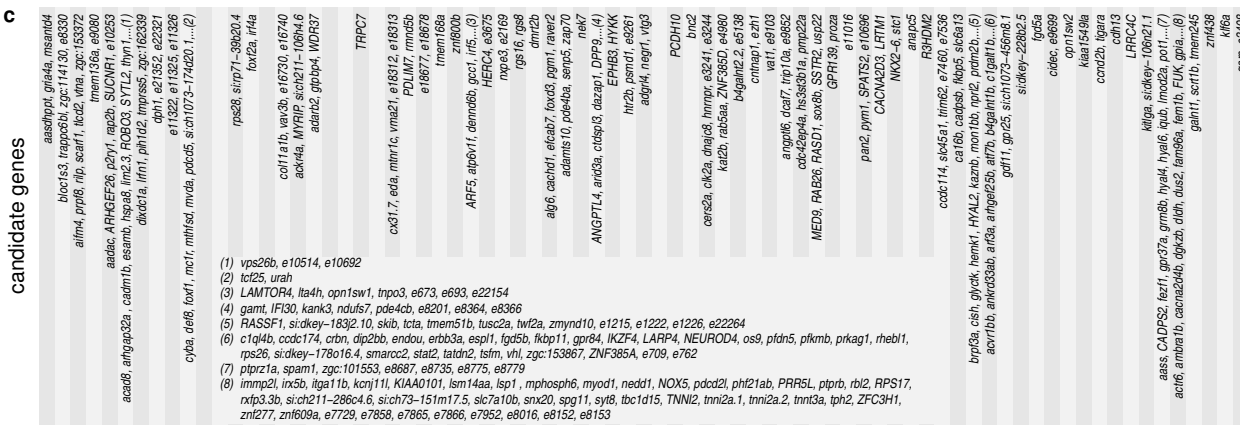
plate count  
plate height  
dorsal spine length  
pelvic spine length  
defence other  
body size  
jaw length  
gill raker number  
gill raker length  
gill raker spacing  
feeding other  
black pigmentation  
behavior  
reproduction  
respiration  
swimming  
body shape

**b**

GE/GP assoc.



vertebrate predators  
lateral plate number  
dorsal spine length  
pelvic spine length  
body size  
jaw length  
gill raker number  
melanism  
light spectrum  
blackwater  
lake area  
genomic PC1

**c**

\*  $p < 0.05$   
\*\*  $p < 0.01$   
\*\*\*  $p < 0.001$

$\beta =$   
11.4 parallel  
5.7  
0  
-5.7  
-11.4 non-par.